PTV and PIV Based Dispersed Phase Velocity Measurements in a Pseudo-2D Turbulent Fluidized Bed

Jari Kolehmainen, Jouni Elfvengren, Markku Ylönen, Pentti Saarenrinne
Tampere University of Technology
Korkeakoulunkatu 6, 33720 Tampere, Finland
jari.2.kolehmainen@tut.fi; jouni.elfvengren@tut.fi; markku.ylonen@tut.fi; pentti.saarenrinne@tut.fi;

Sirpa Kallio, Juho Peltola
VTT Technical Research Centre of Finland
P.O. Box 1000, FI-02044 VTT, Finland
sirpa.kallio@vtt.fi; juho.peltola@vtt.fi

Abstract – Fluidized beds are used in a wide variety of industrial applications ranging from power generation to chemical industry. In a fluidized bed pressurised gas is blown from the bottom of the bed to a solid mass consisting of small particles. The drag force between the gas and the particles causes the bed become fluidized. Fluidized beds can be roughly categorized as bubbling, turbulent, or circulating fluidized beds with increasing fluidization air velocity. In this study, particle velocities and sizes are measured using Particle Tracking Velocimetry (PTV) combined with Particle Image Velocimetry (PIV) in near the top of a turbulent fluidized bed containing two particle populations. In this region the suspension is typically dilute and thus the dispersed phase behaviour is mostly determined by fluid-particle interactions. The dispersed phase velocity measurements were used to compute the time averaged velocity fluctuations and Reynolds stresses. The velocities were categorized by horizontal position, and by measured mass averaged mean fluidization air velocity. The results were compared to few circulating and bubbling fluidized bed studies. The particle velocity profile near the wall was similar to profiles observed in the circulating fluidized bed studies. It was also noticed that the large particles exited the upward flow before smaller particles which lead to differences in comparison to circulating fluidized bed studies. The approach of using a combination of PIV and PTV to handle the varying particle densities was found out to be effective when dealing with flows of highly variable particle densities. In a test case, it was found out that the PIV velocity estimates are slightly less than the corresponding PTV estimated velocities.

Keywords: Fluidized Bed, Particle Tracking Velocimetry (PTV), Particle Image Velocimetry (PIV), Particle Swarm Optimization (PSO), Solid Phase Reynolds Stress.

1. Introduction

Particle Tracking Velocimetry (PTV) offers more detailed information about particle velocities than the cross-correlation based Particle Image Velocimetry (PIV). In PTV the motion of single particles is tracked between sequential images, while PIV provides a most probable velocity for a population of particles in a selected interrogation region. Thus, PIV lacks the ability to determine the number of particles and particle sizes inside the interrogation regions, whereas a PTV algorithm is able to provide this information.

The present article investigates the behaviour of particles with a bimodal size distribution in a pseudo-2D fluidized bed. Results are obtained from upper parts of the fluidized bed at four different superficial air velocities. Typically, PTV algorithms are designed to be used in dilute suspensions with nearly constant seeding density of the flow tracer particles. However, in a fluidized bed the particle density varies substantially both temporally and spatially and the particle motion differs substantially from the fluid motion. Particles may also form clusters and overlap each other. Commonly used PTV algorithms often fail to identify single particles inside clusters containing several particles. In order to detect the motion of individual particles inside clusters, a PTV algorithm utilizing Particle Swarm

Optimization (PSO) was presented by Kolehmainen et al. (2014). Since the dense particle images should not be neglected in the computation of statistical properties, a PIV analysis was coupled with the previously presented PTV algorithm.

1. 1 Background

Many different methods have been used to measure solid particle velocities in fluidized beds. These methods can be divided into intrusive and non-intrusive methods. The non-intrusive methods are able provide detailed information about the particle motions without disturbing the flow. Perhaps the oldest optical non-intrusive measurement technique applied to fluidized beds is Phase Doppler Anemometry (PDA). It allows simultaneous measurement of particle velocity and particle size with high accuracy. PDA has been used for fluidized bed studies for instance in article (Samuelsberg et al., 1996). Unfortunately, PDA cannot supply any information regarding the surroundings of the measurement point due to its nature. Other non-intrusive methods include more recently developed particle field imaging based methods such as PIV and PTV. Unfortunately these methods require clear optical access to the measured flow region, which limits their usability to dilute particle suspensions, near-wall behaviour or pseudo-2D conditions.

If there is optical access, the cross-correlation based PIV method can be applied to analyse dense gas-particle flows, where single particles are difficult to detect, as long as the image texture does not deform too severely in sequential frames. However, good quality PIV requires adequate seeding, which results in a poor performance in dilute suspensions. The inherent noise in the images produces lots of erroneous displacement vectors in regions where no particles are present. These small randomly orientated vectors can be difficult to filter out without also removing valid vectors. PIV has been successfully applied to measurement of particle phase velocities in a pseudo-2D fluidized bed in Kolehmainen et al. (2013), Laverman et al. (2008) and Agarwal et al. (2011).

In comparison to PIV, PTV requires detection of individual particles and performs best in dilute small scale studies. Unlike PIV, PTV cannot be regarded as a single technique but rather a family of algorithms, and there are hundreds of variations in the literature. PTV has been used to measure granular temperature by Jung et al. (2005) and Mehmet et al. (2004). This parameter is used in the kinetic theory of granular flows, and is closely related to dispersed phase Reynolds stresses measured in this article.

1. 2. Scientific Contribution

The dilute top section of a turbulent fluidized bed has not been widely studied in the literature. The authors were unable to find any directly related articles with similar flow conditions. Although not widely studied, this region generates a gas-solid flow with a strongly varying suspension density similar to many practical applications in an easily accessible experimental setup. In this work, the authors have successfully demonstrated the usability of combined PTV-PIV in a semi-dilute gas-particle two-phase flow, and determined averaged particle numbers, velocities, and Reynolds stresses in the upper section of a turbulent fluidized bed.

2. Measurement Setup
2. 1 Overview

The experimental setup consisted of a pseudo-2D fluidized bed filled with sieved spherical class beads with mean diameters of 230 and 390 micrometers and narrow distributions. There was 20 ml of both particle populations. The fluidized bed height was 700 mm and width 100 mm. Distance between the transparent walls was 6 mm making the flow inside the bed nearly two-dimensional.

The inlet air mass flow was measured using a pressure drop measurement over a long feed line. The mass averaged velocity was calculated from the pressure drop measurement to give an estimate of flow velocity. The inlet air velocity was varied during the experiment using a pressure regulator valve.

In order to reduce the effect of static electricity inside the fluidized bed, a humidifier was employed. The humidifier consisted of an air-water cyclone immersed in a hot water bath that kept the temperature constant. The air humidity was measured using an external humidity gauge to ensure that sufficient air

humidity was obtained. It was found that when the humidity was between 75% and 85% the static electricity did not affect the fluidized bed behaviour. The humidity was controlled by altering the water bath temperature. Moreover, addition of moisture in the cyclone had only a minor effect of few percentages on the density of air; hence it was excluded from the calculations.

The particles were illuminated by an expanding laser beam and a diffuser plate placed behind the bed. The particle shadow images were recorded using a high speed video camera. The image location in the fluidized bed was determined from a calibration image with a transparent measurement grid. Five image locations from the left edge to the centre line of the bed at a height of 330 mm from the air distributor were selected. Interrogation regions were divided to image quarters as illustrated in Fig. 1.
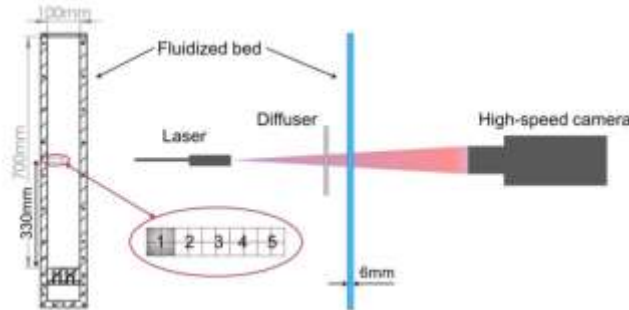

Fig. 1. Illustration of the optical measurement setup.

2. 2 Optical Measurement of Particle Size and Velocity

The particle shadow images were recorded using a Photron SA-5 high speed video camera. The lens used was K2 infinity long-distance microscope that allows a large focal length compared to the image region. The images were illuminated by a Cavitar HF diode laser with a wavelength of 810 nm. The camera recorded a five image sequence from the fluidized bed two times every second. The temporal framerate inside the five image sequence was set to 4,000 fps with a resolution of 1024 x 1024 pixels. Each frame was 10.3 mm wide. Laser pulse width was set to 100 ns which was considerably less than the camera exposure time. Due to the short effective exposure time there was practically no elongation or distortion in the particle images.

From the five image sets only the last two images were used for further processing. The three first images were disposed since there were slight oscillations in the recorded image intensity. The remaining images were divided into two groups by thresholding the average image intensity. The first group consisted of images where the particle concentration was deemed dilute, while the latter consisted of images where there were too many particles for the PTV algorithm. A sample image of each flow group is shown in Fig. 2. The intensity threshold to switch from PTV to PIV in this study was set to 85 while the average background intensity was 114. The grey scale intensity was stored in 8-bit unsigned integers giving a maximum intensity value of 255.
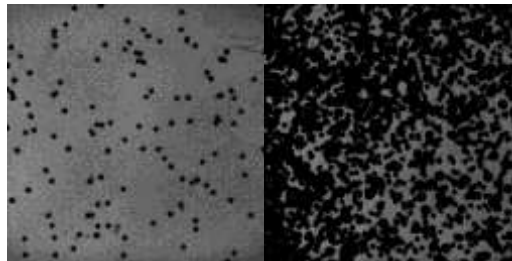

Fig. 2. Left side shows an image of dilute flow conditions with only a few overlapping particles. Right side shows an image of semi-dilute flow conditions where there are lots of overlapping particles.

If the particle concentration in the image was deemed to be dilute, the velocity and the size of each particle were computed using a PTV algorithm presented in Kolehmainen et al. (2014). The applied PTV algorithm could detect particles and measure sizes of particles inside small clusters of particles close to each other which enabled its use even in semi-dilute flow conditions. The particle tracking of the PTV algorithm was carried out using an advanced two frame tracking method presented in the article (Ohmi et al., 2000).

In the images where particle suspension was considered dense, the velocity field was estimated by PIV and the volume fraction from the image intensity. The PIV fields were computed by the PIV software Davis 8.1.3 using multi-pass cross-correlation method with decreasing window size.

Due to the working principle of PIV, the average velocities are not Favre averages (i.e. mass-weighted averages) like the averaged PTV results, but rather volumetric averages where each image subdomain has the same weight independent of the particle number inside the domain. Hence, averages computed by PTV and PIV have slightly different meaning. PIV has also a tendency to blend zero velocities from the background to the estimated velocity field. This behavior causes underestimation of the particle displacement. This difference between averaged results obtained with PTV and PIV is demonstrated in Fig. 3.
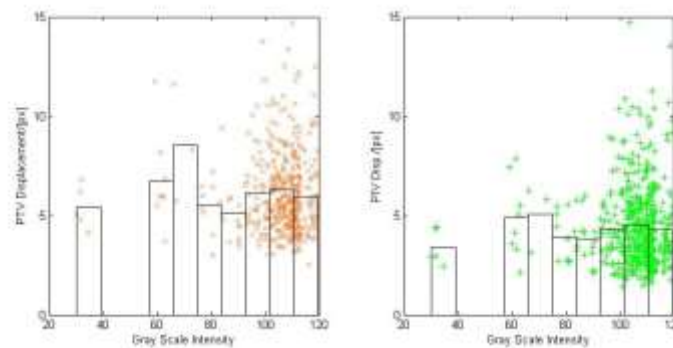

Fig. 3. Figure showing difference in particle displacement estimation by PTV (left) and PIV (right). Black bars show the mean displacement for a given intensity interval and crosses show scatter plots. The plots are generated from measurement data taken from 20mm away from the bed wall with mean air velocity of 3.09m/s.

In the cases of low air mean velocity, the whole measurement set was dilute enough to be analyzed using only PTV. However, at higher air velocities the PIV measurements consisted of a quarter of the total measurements, and therefore had a statistical impact on the results. At the intermediate air velocities the PIV based velocity fields covered about 10 percentages of the total measurements.

2. 3 Mean Air Velocity Measurement

The mass flow in the piping system is determined by measuring the pressure drop in a fixed length of the pipe and by using the Darcy-Weisbach equation given by Eq. (1). The measurement setup is illustrated in Fig. 4. The flow in the pipe is assumed to be turbulent so that the friction coefficient can be calculated by the law of Blasius for a friction coefficient given by Eq. (2).
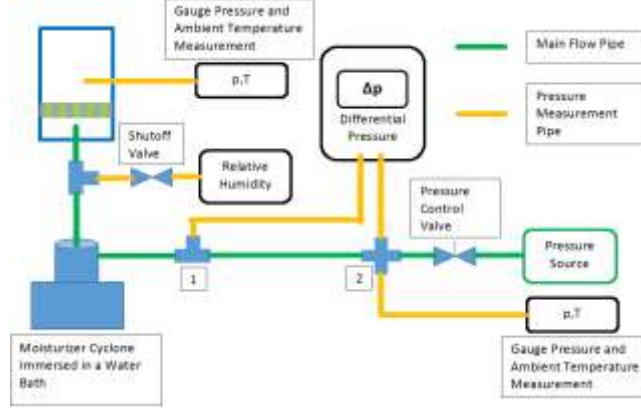
Fig. 4. Schematic illustration of the average air velocity measurement setup.

Darcy-Weisbach equation can be formulated as

$$\Delta p = \frac{1}{2}\xi \rho u^2 \frac{\Delta l}{d}, \tag{1}$$

where the friction coefficient ξ was calculated using Blasius law

$$\xi = \frac{0.3164}{Re^{0.25}} \qquad 4{,}000 < Re < 100{,}000 \tag{2}$$

The Reynolds number in the piping varied from 20,000 to 28,000. Hence the Blasius law should be applicable for the pressure loss through the measurement pipe section. Assuming compressible flow and using the differential form of Eq. (1), the equation for average air velocity in the bed becomes

$$u \approx \frac{1{,}515895 d_{pipe}^{\frac{19}{7}} R^{\frac{-4}{7}} \mu^{\frac{-1}{7}} \Delta l^{\frac{-4}{7}} \left(\frac{p_2^2 - p_1^2}{T}\right)^{\frac{4}{7}}}{\rho A_{bed}}, \tag{3}$$

where the air density ρ was measured from the riser. Notice that R is the specific gas constant of dry air.

3. Results
3. 1 Overview

Each image frame was 10.3 mm wide and five measurement locations were required to cover the fluidized bed from the wall to the centreline of the bed. In addition, in each location measurement sets were recorded at four different air velocities. From each experiment 500 image pairs were recorded and processed. From each processed image pair the particle velocities and sizes were extracted for further post-processing.

Dispersed phase Reynolds stresses can be interpreted as the covariance matrix of velocity computed from a given volume or time interval by Eq. (4) (Crowe et al., 1998). In this study, the volume averaging was done over each quarter of an image. Covariance of random vectors can be computed by

$$\text{cov}(u_i, u_j) = \frac{1}{N-1}\sum_{k=1}^{N}(\overline{u_i} - u_i^k)(\overline{u_j} - u_j^k), \tag{4}$$

where the over bar refers to the respective mean value (time average or volume average), i and j refer to velocity components, k refers to a particle index in volume or to a time instance time averaging and N refers to the total number of samples.

In volume fraction calculation, the particle count was based on particles that the PTV algorithm detected in the first image of the image pair. In the image pairs where PTV could not be applied, the

particle count was estimated by thresholding the image, and counting the area of thresholded particles. The particles area was divided by an average thresholded particle area. This average area was calibrated from a dilute concentration image, where hand counting the particles was possible.

Since this approach cannot distinguish between large and small particles, the particle count computed was assigned to the smaller particles. This is acceptable, since typically there were only few percentages of larger particles from the whole particle count. Moreover, the above mentioned strategy is likely to underestimate the particle count in dense suspensions due to overlapping of the particles.

3. 2 Average Profiles

Time averaged particle counts on 5mm times 10mm measurement areas at various air velocities are shown in Fig. 5. The position is the horizontal distance from the wall, zero being the wall and 50 mm being the centreline of the bed. There was a slight increase in the number of particles near the wall with lower air velocities. The standard deviation of volume fraction increased with increasing number of particles.

Difference from the CFB measurements of Mathiesen et al. (2000) was that the number of large diameter particles increased from the wall to the center line of the fluidized bed. In CFB articles Mathiesen et al. (2000) and Moortel et al. (1998), the particles show opposite behaviour.
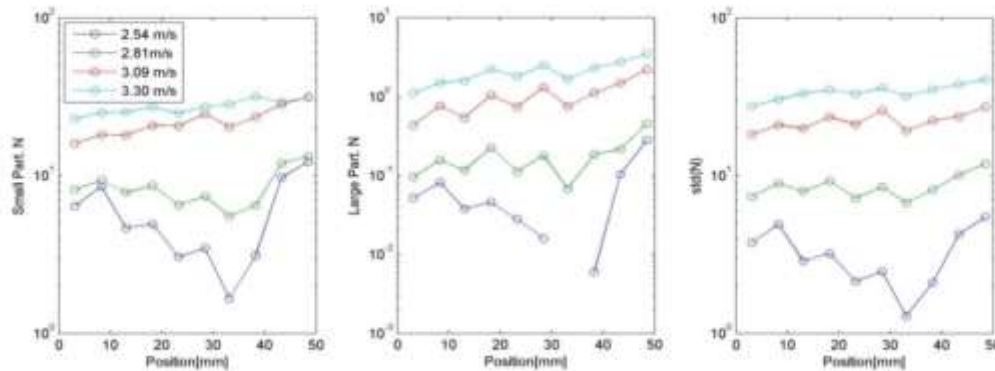

Fig. 5. Time and volume averaged particle number profiles. On the far right the standard deviation of particle count is shown.

The time averaged velocities are shown in Fig. 6. The vertical velocity component is almost zero which is consistent with the fact that the net flux of solids is zero in a turbulent fluidized bed. The horizontal component is negative which suggests that the particles move from the center of the bed to the wall. The hooks observed near the wall have also been reported in CFB experiments, for instance by Mathiesen et al. (2000), and in a BFB study by Laverman et al. (2008). Large particles were excluded due to small sample size that can be seen in Fig. 5.
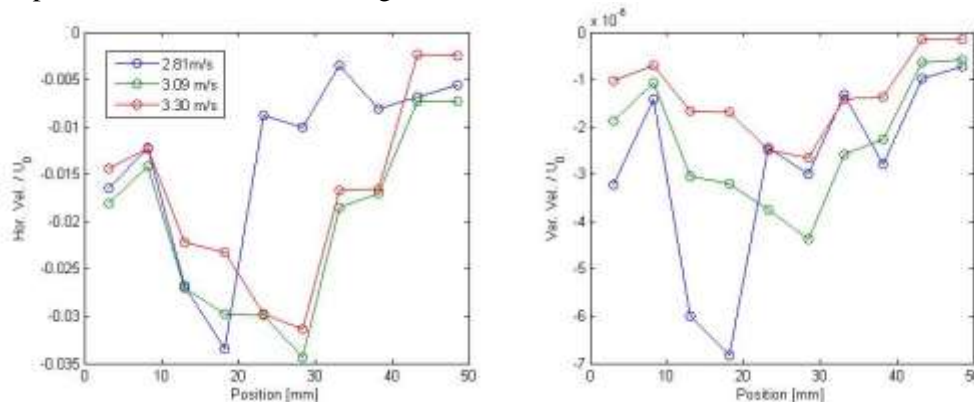

Fig. 6. Time averaged velocity profiles of small particles. Velocities are shown in dimensionless form relative to superficial velocity.

3. 3 Dispersed Phase Reynolds Stresses

Fig. 7 shows velocity fluctuations scaled by the square of the corresponding superficial velocity. The horizontal velocity component fluctuations decrease when approaching the wall. The vertical velocity component fluctuations on the other hand increase when approaching the wall.

Fig. 8 shows the time averages of the superficial velocity scaled dispersed phase Reynolds stresses (Crowe et al., 1998), also called as laminar particle stresses (Mayank et al., 2011) by some authors. The difference between velocity fluctuations of Fig. 7 and the Reynolds stresses of Fig. 8 is that the velocity fluctuations are computed as a covariance matrix (computed with Eq. (4), k refers now to the time instance) of the volume averaged velocities, while Reynolds stresses are time averages of the covariance matrix values computed over a volume at each time instance by Eq. (4) (k is in this case the particle index). The volume considered in the averaging is a quarter of the original image.

Reynolds stresses were computed from the PTV results alone since the PIV velocity fields are much smoother than the PTV fields, and therefore underestimate the Reynolds stresses. The vertical velocity fluctuations and the Reynolds stresses are larger by magnitude than the horizontal velocity fluctuations, demonstrating that the flow is highly anisotropic.
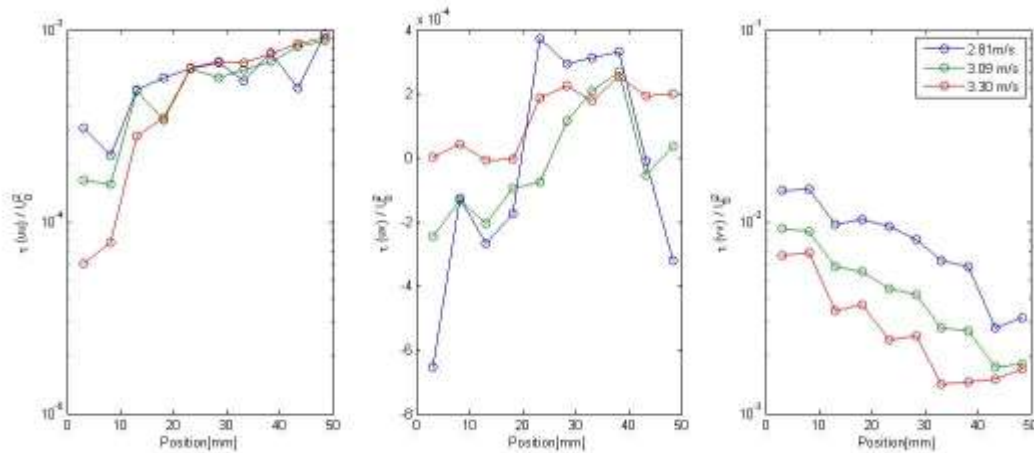

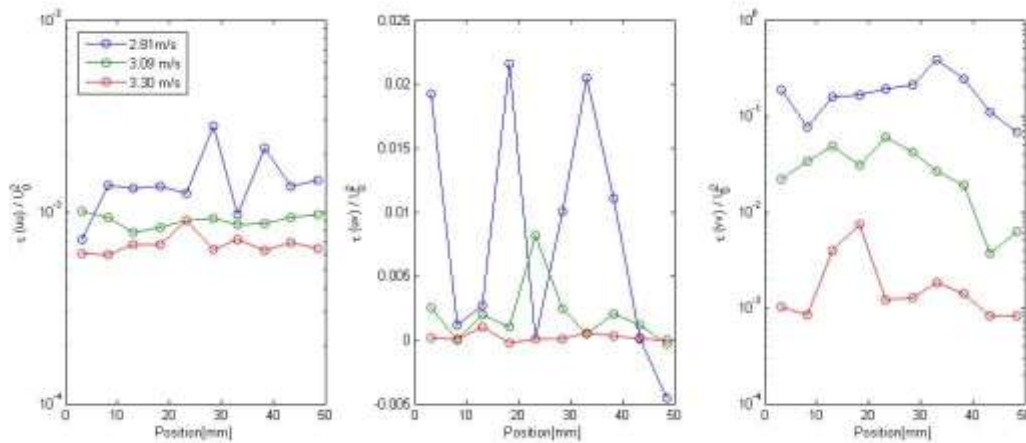Fig. 7. Superficial velocity scaled velocity fluctuations of volume averaged velocities.

Fig. 8. Superficial velocity scaled dispersed phase Reynolds stresses.

4. Conclusion

In this study, mean particle number, time averaged velocities, velocity fluctuations and dispersed phase Reynolds stresses were measured using a combined PTV-PIV method in the dilute top section of a turbulent fluidized bed. There were equal volumetric amounts of two particle populations with different narrow size distributions in the fluidized bed. The velocity results were shown only for the smaller sized

particles (230 μm) since the sample size of the larger sized particles (390 μm) was very small in the measurement height of the bed. Results were compared to bubbling, turbulent, and circulating fluidized beds in order to find similarities and differences between various types of fluidized beds.

In comparison to CFB studies of Mathiesen et al. (2000) and Moortel et al. (1998), the large particle population shows opposite behaviour in a turbulent fluidized bed: the particle number increases from wall to the centre line of the bed. This behaviour is probably caused by large particles exiting the upward gas flow earlier than smaller particles. However, validating this hypothesis would require additional measurements below the measurement section of this study.

The averaged velocity profiles corresponded to the CFB study of Mathiesen et al. (2000) with an exception that the vertical velocity was very close to zero. Interestingly, the velocity profile shape was also similar to a BFB shown in Laverman et al. (2008). In summary, it can be stated that particles descent near the wall and there is a region next to the wall where the descending velocity is largest. Furthermore, there is a region between the wall and the maximum descending velocity region where the particle descending velocity is low. This causes hooks in the velocity profile that were observed in this study, and also in CFB (Mathiesen et al., 2000) and BFB studies (Laverman et al. 2008).

PIV was found out to underestimate the velocities compared to PTV due to zero blending from the background. In addition, PIV produces overly smooth fields that restrict its use to sufficiently smooth fields. For this reason, PIV should not be used for low level Reynolds stress estimation unless adequate resolution is obtained. Regardless of the differences between PIV and PTV, PIV can be used to assist PTV analysis in a valuable way and is certainly better than discarding the frames where PTV cannot be performed.

Acknowledgements

References
Agarwal G., Lattimer B., Ekkad S., Vandsburger U. (2011). Influence of multiple gas inlet jets on fluidized bed hydrodynamics using Particle Image Velocimetry and Digital Image Analysis. Powder Technology, 214, 122–134.

Crowe C.T., Schwarzkopf J.D., Sommerfeld M., Tsuji Y. (2011). Multiphase Flows with Droplets and Particles, Second Edition. CRC Press.

Jung J., Gidaspow D. (2005). Measurement of Two Kinds of Granular Temperatures, Stresses, and Dispersion in Bubbling Beds. Ind. Eng. Chem. Res., 44, 1329–1341.

Kolehmainen J., Elfvengren J., Saarenrinne, P. (2013). A measurement-integrated solution for particle image velocimetry and volume fraction measurements in a fluidized bed. International Journal of Multiphase Flow, 56, 72–80.

Kolehmainen J., Elfvengren J., Saarenrinne, P. (2014). Interference Based Dense Suspension Particle Tracking in Fluidized Beds. Experiments in Fluids. In Review.

Laverman J.A., Roghair I., van Sint Annaland M., Kuipers H. (2008). Investigation Into the Hydrodynamics of Gas–Solid Fluidized Beds Using Particle Image Velocimetry Coupled With Digital Image Analysis. Can. J. Chem. Eng., 86, 523–535.

Mathiesen V., Solberg T., Hjertager B.H. (2000). An experimental and computational study of multiphase flow behavior in a circulating fluidized bed. International Journal of Multiphase Flow, 26, 387–419.

Mayank Kashyap, Benjapon Chalermsinsuwan, Dimitri Gidaspow. (2011). Measuring turbulence in a circulating fluidized using PIV techniques. Particuology, 9, 572–588.

Mehmet T., Gidaspow D. (2004). Measurement of Granular Temperature and Stresses in Risers. AiChe Journal, 50, 1760–1775.

Ohmi K., Li H. (2000). Particle-tracking velocimetry with new algorithms. Measurement Science Technology, 11, 603–616.

Peltola J., Karvonen L., Elfvengren J., Kolehmainen J., Kallio S., Pallarès D., Johnsson F. (2014). Measurement of Solids Velocity and Concentration Distributions in a Large CFB Cold Model. The full-text manuscript was accepted to 11th International Conference on Fluidized Bed Technology (CFB-11) that will be held in Beijing, China, in May.

Pope S.B. (2000). Turbulent Flows. Cambridge University Press.

Samuelsberg A., Hjertager B.H. (1996). An experimental and numerical study of flow patterns in a circulating fluidized bed reactor. International Journal of Multiphase Flow, 22, 575–591.

Van den Moortel T., Azario E., Santini R., Tadrist L. (1998). Experimental analysis of the gas-particle flow in a circulating fluidized bed using a phase Doppler particle analyzer. Chemical Engineering Science, 53, No. 10, 1883–1899.